



Analysis of free-carrier optical absorption used for characterization of microcrystalline silicon films

T. Sameshima^{a,*}, K. Saitoh^a, N. Aoyama^a, M. Tanda^b,
M. Kondo^b, A. Matsuda^b, S. Higashi^c

^a*Tokyo University of Agriculture and Technology, Tokyo 2-24-16 Nakamachi, Kaganei 184-8588, Japan*

^b*Electrotechnical Laboratory, Ibaraki 305-8568, Japan*

^c*SEIKO Epson Corporation, Nagano 392-8502, Japan*

Abstract

The analysis of free-carrier optical absorption was applied to investigation of electrical properties for doped microcrystalline silicon films formed at 100–180°C by the RF-plasma-enhanced chemical vapor deposition method. The analysis gave in-depth characteristics of the carrier mobility and the carrier density. The electron mobility was 8 cm²/Vs (phosphorous doped) and 6 cm²/Vs (boron doped) at the surface region and it decreased to ~ 1 cm²/Vs at bottom film/substrate interfaces. The carrier mobility and density were much higher than those obtained by Hall effect current measurements. It shows the existence of substantial non-activated and disordered regions among crystalline grains. © 2001 Elsevier Science B.V. All rights reserved.

Keywords: Carrier mobility; Carrier density; Disordered states; Free-carrier optical absorption; Hall effect

1. Introduction

Polycrystalline silicon films are important for a variety of applications in many devices such as thin-film solar cells as well as thin-film transistors (TFTs) [1–4]. The electrical current measurements including the Hall effect give the mobility and the density of the carriers which propagate across many grain boundaries in polycrystalline silicon (poly-Si) films. The electrical current suffers from carrier transport properties in both crystalline grains and grain boundaries. We recently reported free-carrier

* Corresponding author.

E-mail address: tsamesim@cc.tuat.ac.jp (T. Sameshima).

optical absorption analysis of thin laser-induced crystallized silicon films [5,6]. Because free-carrier optical absorption occurs via excitation induced by the electrical field of incident photons followed by energy relaxation in the crystalline grains, the analysis gives the carrier mobility and carrier density inside the crystalline grains.

In this paper, we apply the analysis of free-carrier optical absorption to the investigation of electrical properties of doped microcrystalline silicon films, which constitute an important material for solar cells as well as thin-film transistors. We report in-depth profiles of the carrier mobility and carrier density for phosphorous-doped microcrystalline silicon films with different film thicknesses. We also discuss grain boundary properties with the experimental results of free-carrier optical absorption and Hall-effect current measurements. Increases in the carrier mobility and the carrier density caused by pulsed-laser annealing are also presented.

2. Experimental

Phosphorus- and boron-doped microcrystalline silicon films were formed on quartz glass substrates by 100 W-radio frequency (RF) plasma-enhanced chemical vapor deposition method at 180°C with SiH₄, PH₃ (1000 ppm) and H₂ gases at flow rates of 10, 100 and 500 Sccm, respectively and at 100°C SiH₄, B₂H₆ (100 ppm) and H₂ gases at flow rates of 3, 20 and 500 Sccm, respectively. The silicon films were irradiated in vacuum at room temperature by a 28-ns pulsed XeCl excimer laser. Multiple-step-laser energy irradiation was carried out. The laser-energy density was increased from 160 (melting threshold) to 360 mJ/cm² in 20 mJ/cm² steps. Five pulses were irradiated at each laser energy density step.

Optical reflectivity was measured at room temperature in the wave number range between 400 and 4000 cm⁻¹ by conventional Fourier transform infrared spectrometry (FTIR) to analyze optical absorption of free carriers in the doped silicon films. The reflection was detected at a resolution of 4 cm⁻¹. In order to investigate in-depth profiles of the carrier mobility and carrier density, we developed an analysis program of free carrier optical absorption for multiple layered silicon structure, in which the carrier mobility, the carrier density and the crystalline volume fraction can be changed in each layer. The free-carrier optical absorption causes changes in the refractive index as well as in the extinction coefficient [5] as shown by the following equations [6,7]:

$$\varepsilon_1 = n_f^2 - k_f^2 = 1 - \frac{\omega_p^2 \tau^2}{1 + \omega^2 \tau^2}, \quad \varepsilon_2 = 2n_f k_f = \frac{\omega_p^2 \tau}{\omega(1 + \omega^2 \tau^2)},$$

$$n_f = \frac{1}{\sqrt{2}} \left[n_{\text{Si}}^2 - A + \left\{ (n_{\text{Si}}^2 - A)^2 + \frac{A^2 e^2}{4\pi^2 m^2 c^2 \mu^2 K^2} \right\}^{0.5} \right]^{0.5},$$

$$k_f = \frac{1}{\sqrt{2}} \left[A - n_{\text{Si}}^2 + \left\{ (n_{\text{Si}}^2 - A)^2 + \frac{A^2 e^2}{4\pi^2 m^2 c^2 \mu^2 K^2} \right\}^{0.5} \right]^{0.5},$$

$$A = Nm\mu^2 \varepsilon_0^{-1} (1 + 4\pi^2 m^2 \mu^2 c^2 e^{-2} K^2)^{-1}, \quad (1)$$

where c is the velocity of light in vacuum, e is the electrical charge, m is the effective mass of the carrier, whose dependence on the carrier density was determined by Miyao et al. [8], τ is the carrier lifetime, ω is the angular frequency and ω_p is the plasma frequency, ε_1 is the real part of the dielectric constant, ε_2 is the imaginary part of the dielectric constant, K is the wave number, μ is the carrier mobility, N is the carrier density and n_{si} is the refractive index of undoped crystalline silicon. The experimental spectra were compared to the spectra obtained by the interference calculation of the multiple layer with the refractive index, n_f , and the extinction coefficient of silicon, k_f , given by Eq. (1) by changing the values of the parameters of carrier mobility and carrier density until the best coincidence of those spectra was obtained. Because the free-carrier optical absorption occurs in crystalline grains, the carrier mobility and carrier density inside crystalline grains are obtained by the analysis of the optical absorption. The Hall effect measurements by the van der Pauw method were carried out at room temperature for silicon films with an area of $5\text{ mm} \times 5\text{ mm}$ with Al electrodes formed at each corner to obtain the carrier mobility and the carrier density. The Hall mobility, μ_H , is deduced from the relation, $\mu_H = R_H \sigma = r_H \mu_D$, where R_H is the Hall constant, σ is the electrical conductivity, r_H is the Hall scattering factor and μ_D is the drift mobility.

3. Results and discussion

Fig. 1 shows the experimental spectra for the as-deposited phosphorus-doped microcrystalline silicon films with different film thicknesses of 70, 140 and 380 nm. Fig. 1 also shows the calculated spectra, which agreed well with the experimental ones. The experimental and calculated spectra show different curves indicating different degrees of free-carrier optical absorption, which depends on film deposition conditions. Fig. 2 shows in-depth dependencies of the carrier mobility (a) and (c) and

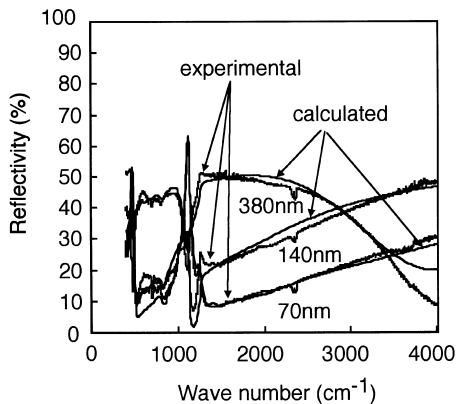


Fig. 1. Experimental spectra for as-deposited phosphorus-doped microcrystalline silicon films with different film thicknesses of 70, 140 and 380 nm and the calculated spectra fitted to experimental ones.

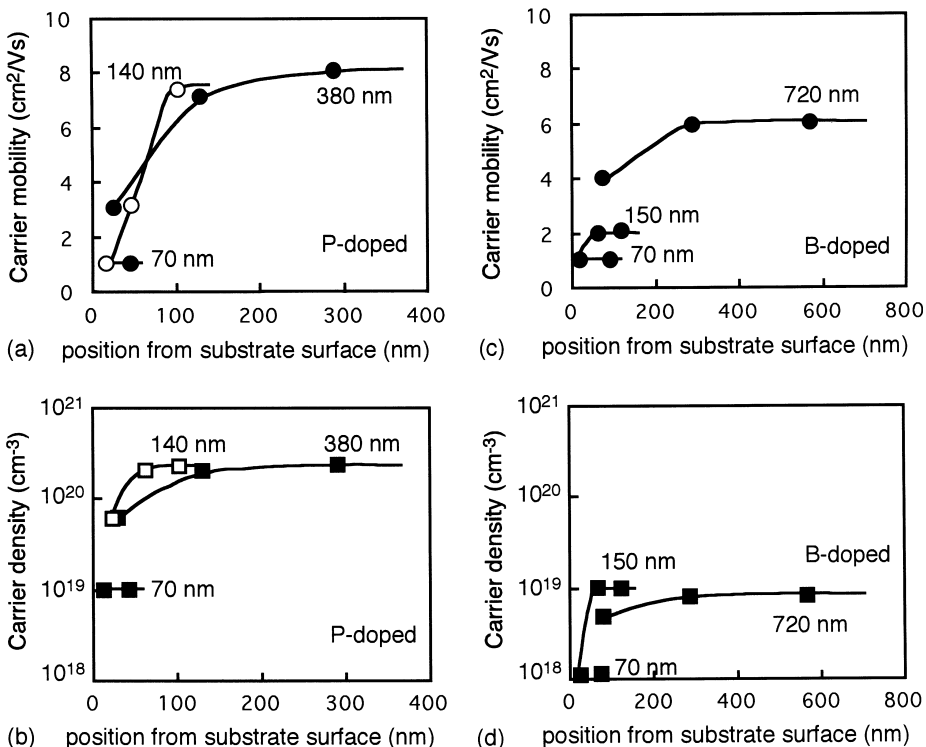


Fig. 2. In-depth profiles of the carrier mobility and the carrier density obtained by the analysis of free-carrier optical absorption. (a) and (c) are carrier mobility for phosphorus-doped films with different film thicknesses. (b) and (d) are the carrier density for boron-doped films.

the carrier density (b) and (d) obtained by the analysis of free-carrier optical absorption for phosphorus- and boron-doped films with different film thicknesses, respectively. The carrier mobility was about 1 cm²/Vs just above the substrate. This means that crystalline properties just above the substrate were not good for phosphorus-doped silicon films and there was substantial density of defect states, which reduced the carrier mobility. The carrier mobility increased to 8 cm²/Vs at the surface region for 140 and 380 nm thick films. The carrier mobility was about 6 cm²/Vs at the surface region for 720 nm thick silicon films. The carrier density was 2.2–2.3 × 10²⁰ cm⁻³ near the surface region although it was lower than 1 × 10²⁰ cm⁻³ near substrates for 140 and 380 nm thick films. Crystalline states and the dopant activation ratio were improved as the film thickness increased. Similar results were obtained for boron-doped silicon films although the carrier density was lower than that of phosphorus-doped silicon because of film deposition conditions. The carrier density was about 10¹⁹ cm⁻³ near the surface region for 150 and 720 nm thick silicon films.

Fig. 3 shows the average carrier mobility (a) and (c) and the average carrier density (b) and (d) obtained by analyses of free-carrier optical absorption and Hall effect

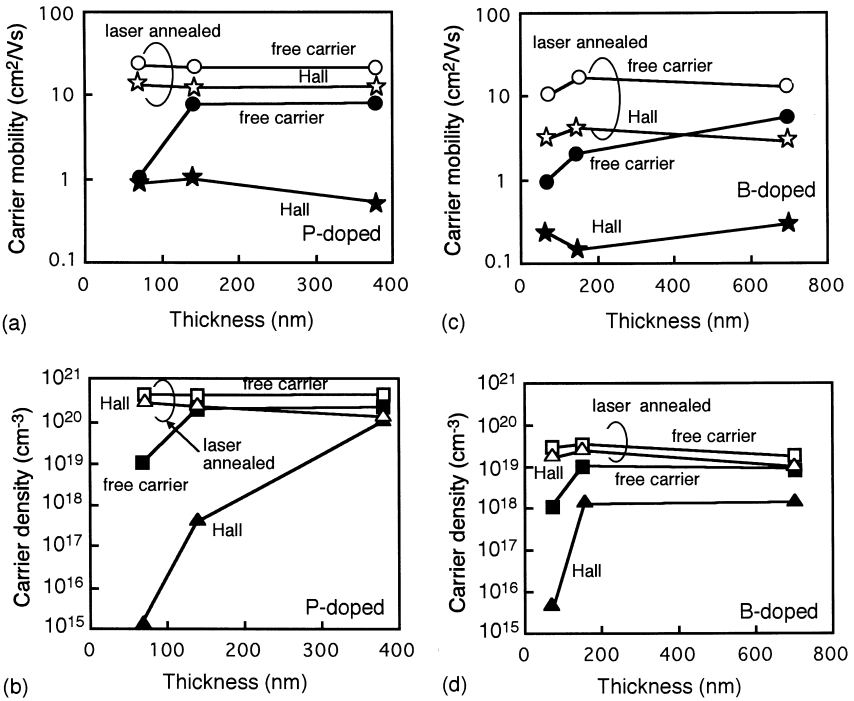


Fig. 3. The average carrier mobility and the average carrier density obtained by analyses of free-carrier optical absorption and Hall-effect current measurements as a function of film thickness for the as-deposited and laser crystallized at 360 mJ/cm². (a) and (c) are carrier mobility for phosphorus-doped films with different film thicknesses and (b) and (d) are the carrier density for boron-doped films.

current measurements as a function of film thickness for phosphorus- and boron-doped films. Fig. 3 also shows the average carrier mobility and the average carrier density after laser irradiation with an energy density of 360 mJ/cm², which caused melting of silicon films for about 150 ns and then rapid recrystallization for each silicon film. For the as-deposited phosphorus- and boron-doped films, the carrier mobility obtained by Hall effect current measurements. This result indicates that there were serious defects or high potential barriers at grain boundaries because the electrical current traverses grain boundaries as well as crystalline grains. The free carriers would be scattered at the disordered grain boundaries or reduced by potential barriers at the boundaries. The carrier density obtained from free-carrier optical absorption was also higher than that obtained by Hall effect current measurements for every sample. The difference between the carrier densities obtained by the two kinds of methods decreased as the film thickness increased. These results indicate that crystalline grains with a high mobility and a high free carrier density were formed ~ 100 nm near the substrate. However, low carrier density measured by the Hall effect current means that there were substantial disordered states with dopant atoms not activated between crystalline grains especially for films thinner than 100 nm. The

amount of these disordered states decreases the electrical conductivity in the lateral direction so that the electrical current traversing between crystalline grains became low. The amount of disorder was reduced as the film thickness increased and the silicon film became much more conductive. Laser irradiation increased carrier mobility and the carrier density obtained by free-carrier optical absorption analyses and Hall-effect measurements for phosphorus-doped and boron-doped silicon film for all film thicknesses. Increase in the carrier mobility means that crystalline properties were improved by laser irradiation. There is still substantial density of defect states in crystalline grains for as-deposited. The carrier mobility and carrier density obtained by Hall effect measurements were close to those obtained by free-carrier optical absorption after laser irradiation. This means that the grain boundary properties were also improved by laser irradiation. Disordered states and potential barrier height would be reduced by the laser irradiation with an energy density of 360 mJ/cm^2 . This experiment revealed that good crystalline grains with rather high carrier mobility could be formed by plasma-enhanced CVD method. But crystalline properties were not perfect because the carrier mobility was increased by pulsed laser annealing. The electrical conductivity in the lateral direction was seriously reduced due to poor grain boundaries especially for thin silicon films. The laser annealing improved grain boundary properties. The CVD process technology has to solve the problem of conductive grain boundary formation.

4. Summary

We analyzed free-carrier optical absorption of phosphorus- and boron-doped microcrystalline silicon films formed at $100\text{--}180^\circ\text{C}$ by the RF plasma-enhanced chemical vapor deposition method. Optical reflectivity spectra in infrared regions are fitted well by calculated spectra with parameters of the carrier mobility and the carrier density. The analysis gave in-depth characteristics of the carrier mobility and the carrier density. The electron mobility was $8 \text{ cm}^2/\text{Vs}$ (phosphorus doped) and $6 \text{ cm}^2/\text{Vs}$ (boron doped) at the surface region and it decreased to $\sim 1 \text{ cm}^2/\text{Vs}$ at bottom film/substrate interfaces because the crystalline ratio was low near the substrate. The carrier mobility and density were much higher than those obtained by Hall-effect current measurements. It shows that there was non-activated and disordered regions among crystalline grains, which reduced electrical conductance to the lateral direction. Pulsed laser irradiation with an energy density of $360 \text{ cm}^2/\text{mJ}$ increased the carrier mobility and the carrier density. The carrier mobility increased to $20 \text{ cm}^2/\text{Vs}$ for free-carrier optical absorption. Crystalline properties were improved by laser annealing. The grain boundary also became much more conductive after laser irradiation because the Hall mobility and the carrier density were also increased.

Acknowledgements

We thank Dr. T. Watanabe for his support.

References

- [1] T. Sameshima, S. Usui, M. Sekiya, *IEEE Electron Device. Lett.* 7 (1986) 276.
- [2] A. Kohno, T. Sameshima, N. Sano, M. Sekiya, M. Hara, *IEEE Trans. Electron Devices* 42 (1995) 251.
- [3] A. Matsuda, *J. Non-Cryst. Solids* 59-60 (1983) 767.
- [4] Y. Chida, M. Kondo, A. Matsuda, *J. Non-Cryst. Solids* 198-200 (1996) 1121.
- [5] T. Sameshima, K. Saitoh, M. Satoh, A. Tajima, N. Takashima, *Jpn. J. Appl. Phys.* 36 (1997) L1360.
- [6] T. Sameshima, K. Saitoh, N. Aoyama, S. Higashi, M. Kondo, A. Matsuda, *Jpn. J. Appl. Phys.* 38 (1999) L1892.
- [7] H. Engstrom, *J. Appl. Phys.* 51 (1980) 5245.
- [8] M. Miyao, T. Motooda, N. Natuaki, T. Tokuyama, in: *Proceedings on Laser and Electron-Beam Solid Interactions and Materials Processing Elsevier, North-Holland, Amsterdam, 1981, p. 163.*